Tropical water vapour in the lower stratosphere and its relationship to tropical/extratropical dynamical processes in ERA5

Received: 29 August 2019 | Revised: 17 March 2020 | Accepted: 30 March 2020

DOI: 10.1002/qj.3801

Quarterly Journal of the Royal Meteorological Society RMetS

RESEARCH ARTICLE

Tropical water vapour in the lower stratosphere and its relationship to tropical/extratropical dynamical processes in ERA5

Tongmei Wang[1,2] | Qiong Zhang[2] | Abdel Hannachi[1] | Toshihiko Hirooka[3] | Michaela I. Hegglin[4]

[1]Department of Meteorology, Stockholm University, Stockholm, Sweden

[2]Department of Physical Geography, Stockholm University, Stockholm, Sweden

[3]Department of Earth and Planetary Sciences, Kyushu University, Fukuoka, Japan

[4]Department of Meteorology, University of Reading, Reading, UK

Correspondence
T. Wang, Department of Meteorology, Stockholm University Svante Arrhenius Väg 16C, 106 91 Stockholm, Sweden
Email: tongmei.wang@misu.su.se

Funding information
KAKENHI, Grant/Award Numbers: JP18H01270, JP16H04052, JP18H01280; Swedish National Space Board project Dnr 88/11 "Atmospheric modelling using space -based observations of stable water isotopes

Abstract

Stratospheric water vapour (SWV), in spite of its low concentration in the stratosphere as compared to the troposphere, contributes significantly to the surface energy budget and can have an influence on the surface climate. This study investigates the dynamical processes that determine SWV on interannual to decadal time-scales. First, we evaluate two SWV reanalysis products and show that SWV is better represented in a new-generation reanalysis product, ERA5, than in its predecessor, ERA-Interim. In particular, it is shown that SWV in ERA5 is highly consistent with observational data obtained from the SPARC Data Initiative Multi-Instrument Mean (SDI MIM). Second, we investigate the variability of tropical SWV and its relationship to dynamical stratospheric variables. The analyses show that the interannual variability in the tropical lower-stratospheric water vapour is closely linked to the tropical Quasi-Biennial Oscillation (QBO). When westerlies occupy the middle stratosphere and easterlies the lower stratosphere, a decrease is observed in lower-stratospheric water vapour due to a colder tropical tropopause and a QBO-induced enhanced residual circulation. On decadal time-scales, the composite analysis of the boreal winter in two typical periods shows that less SWV is related to a warm anomaly in the North Atlantic sea-surface temperature, which leads to stronger upward propagation of planetary wave activity at high latitudes, a weaker polar vortex and an enhanced residual circulation. The opposite occurs during periods with higher concentrations of SWV.

KEYWORDS

ERA5, planetary wave activity, Quasi-Biennial Oscillation, stratospheric dynamical processes, stratospheric water vapour

1 | INTRODUCTION

Water vapour in the atmosphere is one of the main greenhouse gases and is also a valuable trace gas. It affects atmospheric dynamics and thermodynamics by modulating the radiative forcing directly (e.g., Forster and Shine, 2002; Solomon *et al.*, 2010; Riese *et al.*, 2012) and influences the radiation budget by modulating stratospheric ozone chemistry (Vogel *et al.*, 2011). Although the concentration of water vapour is much lower in the stratosphere than in the troposphere, it has a significant effect on the climate at the surface. Studies using climate models have shown that the increase of stratospheric water vapour (SWV) can have an impact on atmospheric temperatures from the stratosphere all the way down to the Earth's surface (Riese *et al.*, 2012). Forster and Shine (1999) compared the equilibrium temperature response to CO_2 increases, stratospheric ozone loss and SWV increases since 1979, and found that cooling in the upper stratosphere is caused by the increase of CO_2, while ozone loss and water vapour increases are more effective at cooling the lower stratosphere. Increasing SWV induces a stratospheric cooling during 1980s, which is about 30-50% of the observed cooling in the stratosphere **(**Dvortsov and Solomon, 2001). Solomon *et al.* (2010) attributed about 30% of the decadal rate of surface warming during 1990s to increased SWV between 1980 and 2000. Using simulations of the atmosphere-only Community Earth System Model (CESM), Wang *et al.* (2017) concluded that an abrupt drop in SWV produces a global mean surface cooling event, suggesting that a persistent change in SWV could have contributed to the observed hiatus in global warming after 2000.

Due to an increase in the volume of observations of SWV and other stratospheric trace gases from aircraft, balloon-borne instruments and satellite instruments in recent decades, our understanding of stratospheric processes has greatly improved. Furthermore, studies of SWV can provide an improved perspective for understanding global climate change driven by changes in the stratosphere (e.g., Solomon *et al.*, 2010; Dessler *et al.*, 2013; Hegglin *et al.*, 2014; Wang *et al.*, 2018). However, observations from satellites and other remote sensors are limited due to their incomplete temporal and spatial coverage. In such cases, reanalysis data that combine available observations using data assimilation systems and atmospheric modelling can be useful supplements. These widely used reanalysis systems produce estimates of SWV depending on the choice of assimilated observations and representations of key processes that influence the distribution of SWV, such as methane oxidation in the stratosphere that produces water vapour, the freeze-drying effect of air entering the stratosphere and the Brewer–Dobson circulation that affects water vapour transport (Mote *et al.*, 1996). Davis *et al.* (2017) evaluated data for water vapour and ozone in the stratosphere from nine reanalysis products, including the ERA-40 and ERA-Interim products from the European Centre for Medium-Range Weather Forecasts (ECMWF) (Dethof and Hólm, 2004; Dee *et al.*, 2011). They showed that the non-assimilation of SWV observations and deficiencies in the physical representation of stratospheric transport in reanalyses resulted in substantial discrepancies between observational and reanalysis estimates of SWV. Hence the SWV data from these reanalyses may not be suitable for scientific investigation (Davis *et al.*, 2017).

Recently, as part of the Copernicus Climate Change Service (C3S, 2017), the ECMWF released a new atmospheric reanalysis product, ERA5, which covers the period from 1979 to the present. ERA5 featured important changes including higher spatial and temporal resolutions relative to ERA-Interim, as well as updates to the atmospheric model and data assimilation system. The atmospheric model incorporates climate forcings, for example, Coupled Model Intercomparison Project 5 (CMIP5) greenhouse gases, volcanic eruptions, sea-surface temperature (SST) and sea ice cover. Some notable changes that affect SWV directly include that parameterization of supersaturation with respect to ice in cloud-free portions of grid cells has been extended to all temperatures below 273 K (as opposed to only temperatures below 250 K in ERA-Interim) and a more consistent treatment of potentially negative water vapour values in the stratosphere. The data assimilation system includes various newly reprocessed observational datasets from recent instruments that were not assimilated into ERA-Interim; for example, some ozone retrievals from different satellites are used in ERA5, and reprocessed all-sky radiances from Meteosat Second Generation have replaced earlier clear-sky radiance products (Hersbach *et al.*, 2018). These are all related to the SWV through their effects on tropopause temperatures and result in improvements to the representation of SWV in ERA5.

Another advantage the reanalysis data have over observations is that they provide a complete picture of the physical and dynamical processes for the troposphere and middle stratosphere. These processes help us to understand the distribution of stratospheric tracers. For example, the water vapour mixing ratio in the lower stratosphere is determined by microphysical processes at the tropical cold-point tropopause that act on tropical air masses as they pass through the tropical tropopause layer into the stratosphere within the Brewer–Dobson circulation (Brewer, 1949; Hoskins, 1991; Holton *et al.*, 1995). Once the water vapour in the tropical troposphere has condensed to form cumulus clouds due to upwelling within

the Hadley circulation, most of the remaining water content is frozen out because of the extremely cold tropical tropopause temperatures (Fueglistaler *et al.*, 2009). Above the middle stratosphere, water vapour levels gradually increase due to the oxidation of methane. Stratospheric transport is dominated by mean diabatic advection, such as upwelling in the tropics and downwelling in the surf zone at higher latitudes, and together with mixing determines the global-scale distribution of tracers including water vapour (Plumb, 2002). If the SWV is well represented in the reanalysis data, it can help us to better understand the relevant processes that influence SWV.

In this paper, we first evaluate the representation of SWV in the new ERA5 reanalysis by comparing its climatological distribution and seasonal cycle to those of ERA-Interim and satellite observations. We then use the ERA5 dataset to investigate the variability of tropical water vapour in the lower stratosphere and its relation to tropical and extratropical dynamic processes. The manuscript is organized as follows. Section 2 describes the data and methodology. Section 3 presents the results, which are then discussed in section 4. Conclusions are given in the final section.

2 | DATA AND ANALYSIS APPROACH

The SWV in the ERA5 and ERA-Interim ECMWF reanalyses are compared in this study. The complete set of hourly ERA5 data was made available via the Copernicus Climate Change Service Climate Data Store (CDS) in January 2019. Both the ERA5 and ERA-Interim archives feature about 40 years of climate data starting from 1979. An overview of the differences between ERA5 and ERA-Interim is introduced; see also Hersbach *et al.* (2018). We further analyse the atmospheric circulation by using ERA5 data, which consist of daily fields of zonal and meridional wind, temperature, specific humidity, vertical velocity and geopotential height, with a re-gridded horizontal resolution of $1^\circ \times 1^\circ$ (the original spatial resolution of the ERA5 model is 31 km globally, T639), distributed over 137 model levels extending from the surface up to a height of 80 km. A Fourier transform analysis is used to separate the variability into interannual (≤8 years) and decadal (≥9 years) scales.

To evaluate the SWV in the reanalysis data, we use the observed SWV from the SPARC Data Initiative Multi-Instrument Mean (SDI MIM) of stratospheric limb sounders (Hegglin *et al.*, 2013; Hegglin *et al.*, 2014). Here we use a combination of eight SDI water vapour products from the limb-viewing satellite instruments SAGE II, HALOE, POAM III, SAGE III, MIPAS, ACE-FTS, Aura-MLS and SAGE III (ISS). These offer the potential for great improvements over previous model measurement comparisons based on the HALOE dataset only. The SDI MIM used here has a temporal coverage of 1986–2017.

The stratospheric mean meridional circulation is a transport circulation commonly referred to in the literature as the Brewer–Dobson circulation (BDC) (e.g., Plumb, 2002; Shepherd, 2007). Following the definition of Andrews *et al.* (1987), the transformed Eulerian-mean (TEM) residual circulation $(\overline{v}^*, \overline{w}^*)$ is given by

$$\overline{v}^* \equiv \overline{v} - \frac{1}{\rho_0}\frac{\partial}{\partial z}\left(\frac{\rho_0 \overline{v'\theta'}}{\partial\overline{\theta}/\partial z}\right) \tag{1}$$

$$\overline{w}^* \equiv \overline{w} + \frac{1}{a\cos\phi}\frac{\partial}{\partial\phi}\left(\frac{\cos\phi \overline{v\prime\theta'}}{\partial\overline{\theta}/\partial z}\right) \tag{2}$$

where $\overline{v}$ and $\overline{w}$ are the zonal means of the meridional and vertical velocities, respectively. ρ_0, θ, a, z and ϕ represent air density, potential temperature, the Earth's radius, height and latitude, respectively. A bar and prime denote the zonal mean and the perturbation to it.

The wave activity flux (WAF) is conventionally used to analyse propagating planetary waves in three-dimensional space from the troposphere to the stratosphere. The WAF vector (F_s) defined on the sphere is calculated in log-pressure coordinates (Plumb, 1985) and takes the form

$$F_s = p\cos\phi\begin{pmatrix} \frac{1}{2a^2\cos^2\phi}\left[\left(\frac{\partial\psi'}{\partial\lambda}\right)^2 - \psi'\frac{\partial^2\psi'}{\partial\lambda^2}\right] \\ \frac{1}{2a^2\cos\phi}\left[\frac{\partial\psi'}{\partial\lambda}\frac{\partial\psi'}{\partial\phi} - \psi'\frac{\partial^2\psi'}{\partial\lambda\partial\phi}\right] \\ \frac{2\Omega^2\sin^2\phi}{N^2 a\cos^2\phi}\left[\frac{\partial\psi'}{\partial\lambda}\frac{\partial\psi'}{\partial z} - \psi'\frac{\partial^2\psi'}{\partial\lambda\partial z}\right] \end{pmatrix} \tag{3}$$

where p is pressure and ϕ, λ and z are latitude, longitude and height, respectively. A prime denotes perturbations to the zonal-mean field, and ψ, Ω, a and N represent the stream function, the Earth's rotation rate, the radius of the Earth and the buoyancy frequency, respectively. Daily data on circulation variables from ERA5 are used for the calculation of daily F_s, and we then consider the monthly averages of the obtained fields.

3 | RESULTS

3.1 | Comparison of overall features of SWV in observation and reanalyses

Figure 1 shows the SWV climatologies from SDI MIM and the ERA5 and ERA-Interim reanalysis products. The climatological distributions of SWV in the boreal winter (DJF

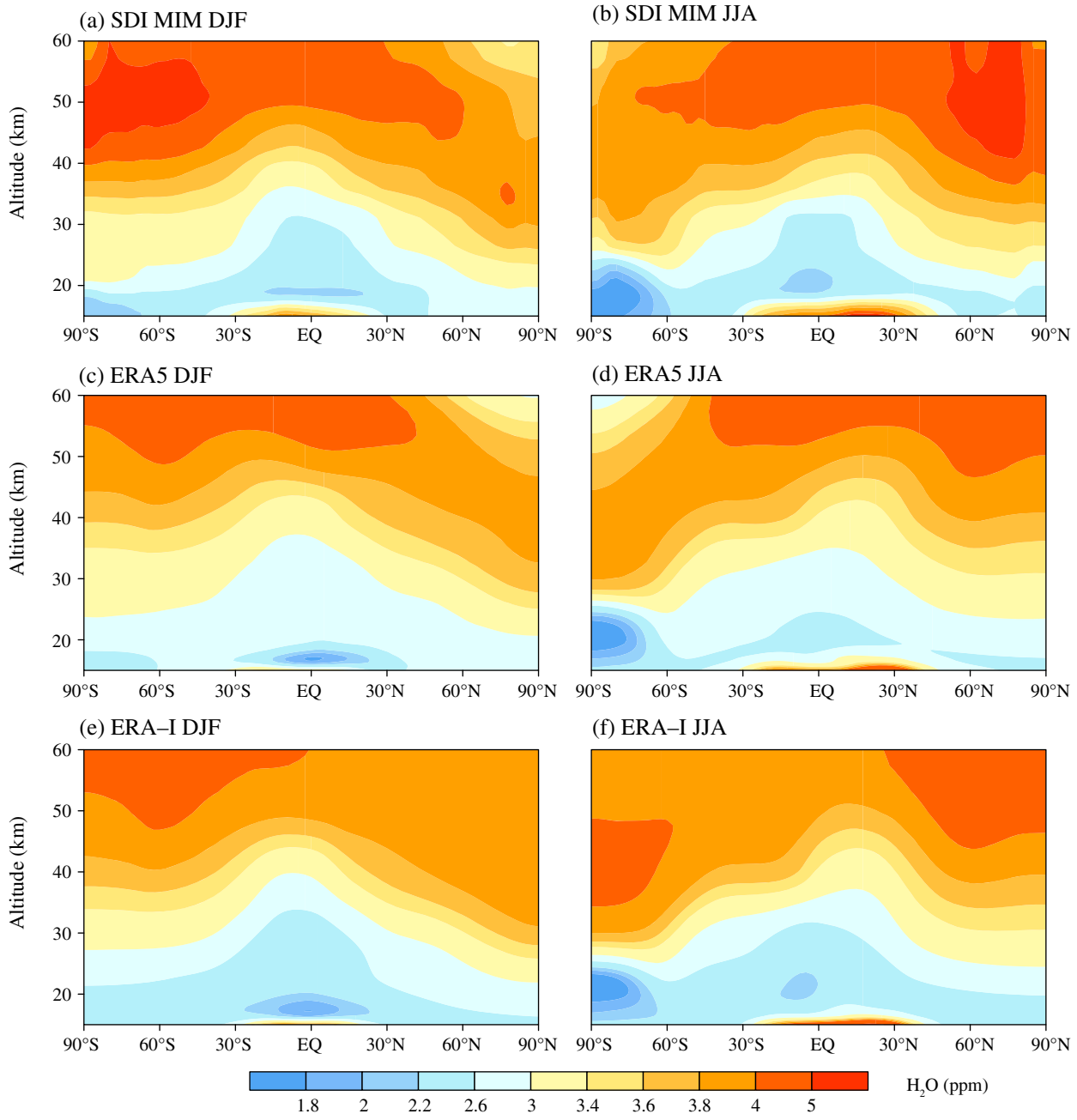

FIGURE 1 Climatological seasonal mean stratospheric water vapour (SWV; shading) for DJF (left column) and JJA (right column) from (a, b) SPARC Data Initiative Multi-Instrument Mean (SDI MIM), (c, d) ERA5 and (e, f) ERA-Interim

mean) and summer (JJA mean) show similar patterns: the lowest values are observed in the lower stratosphere centred over the tropics due to the dehydration of air masses upon entry into the stratosphere through the cold tropical tropopause. Over the tropics and summer hemisphere, SWV increases with height, mainly due to methane oxidation occurring in the upper stratosphere. Over high latitudes in summer, a maximum is located around 50 km in the upper stratosphere in SDI MIM (Figure 1a,b), or around 60 km in the lower mesosphere in both reanalyses (Figure 1c–f). This implies that the methane oxidation layer is higher in the reanalyses than in real-world observations. Since ERA5 has a higher model top (up to 80 km) than ERA-Interim (up to 60 km), the methane oxidation layer is shown more clearly in ERA5 than in ERA-Interim.

During winter in both hemispheres, a local maximum in SWV is found around 40 km in the middle stratosphere for SDI MIM and ERA5 (Figure 1a–d). The local maximum found in water vapour has previously been pointed out by Hegglin *et al.* (2013), with lower values above this region driven by the downward motion from the upper branch of the BDC, bringing very dry air down from the

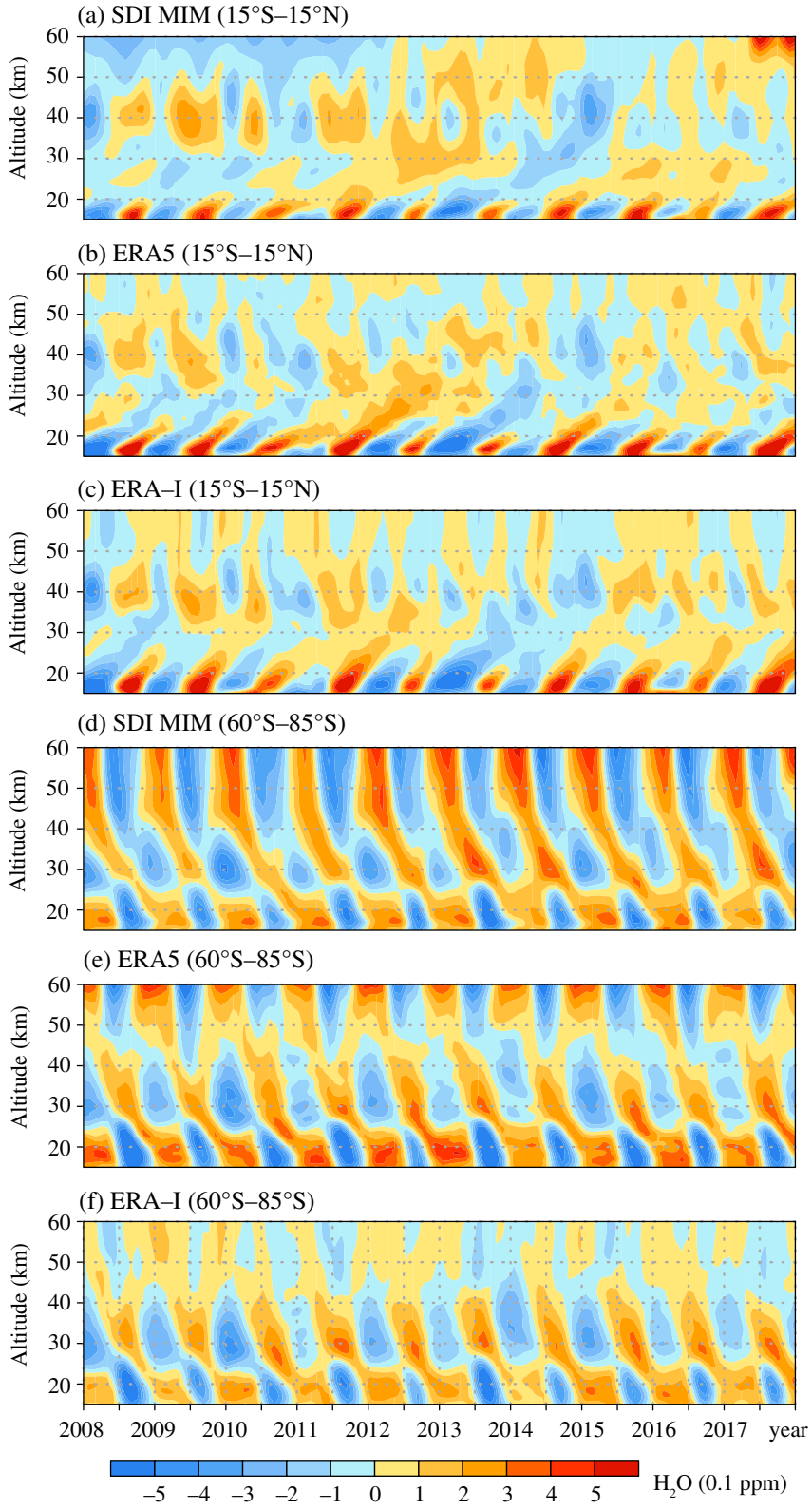

FIGURE 2 Variations in the vertical structure of SWV anomalies from the climatological annual mean: (a, b, c) the tropics (15°S–15°N mean) and (d, e, f) the southern polar region (60°S–85°S mean) using (a, d) SDI MIM, (b, e) ERA5 and (c, f) ERA-interim, respectively. Unit: 0.1 ppm

lower mesosphere and upper stratosphere. This is also consistent with observations from Odin/SMR (Orsolini *et al.*, 2010). In ERA-Interim, this local maximum in the winter hemisphere is observed in JJA (Figure 1f) but not in DJF (Figure 1e). A belt of high values of SWV in the upper stratosphere from the summer to the winter hemisphere (transport via the upper branch of the BDC) shows up clearly in ERA5 (Figure 1c,d) but not in ERA-Interim (Figure 1e,f). These climatological features shown in different datasets indicate that ERA5 provides a

better representation of processes and water vapour in the middle atmosphere.

Figure 2 shows seasonal variation in vertical SWV anomalies (relative to the climatological annual mean distribution) over the tropics and the southern polar region over a 10 year period (2008–2017). In the tropics (Figure 3a–c), the well-known phenomenon of the tropical "tape recorder" is shown in the lower stratosphere in both the observation and reanalysis products. The wet and dry signals propagate upward from the tropopause to the lower stratosphere, which is also seen in other satellite observations and model simulations (Mote *et al.*, 1996; Steinwagner *et al.*, 2010; Hegglin *et al.*, 2013; Eichinger *et al.*, 2015; Wang *et al.*, 2018). Over the southern polar region (Figure 3d–f) the anomaly in SDI MIM shows a distinct wet summer/dry winter contrast in the upper stratosphere resulting from enhanced methane oxidation in the persistently sunlit summer stratosphere. This feature, along with a similar anomaly pattern in the lower stratosphere (below 20 km) and the opposite anomaly pattern in the middle stratosphere, constitutes a triple vertical structure over the polar region. The structures in ERA5 show very similar features. This finding is consistent with the satellite Odin/SMR data on stable water isotopes (Wang *et al.*, 2018). However, in ERA-Interim the anomalies above 40 km are very weak.

On the other hand, we can observe signals of the semi-annual oscillation (SAO) in the tropical upper stratosphere above about 35 km in both reanalyses with minima around February and August, which is consistent with earlier observations (e.g., Jackson *et al.*, 1998). However, these signals might be significantly modulated to show irregular interannual changes due to other processes such as the QBO, sudden stratospheric warmings (SSWs), and the tropical "tape recorder".

In summary, in terms of its climatology and seasonal variations, the SWV is much better represented in ERA5 than in the ERA-Interim reanalysis. ERA5 thus provides an appropriate tool for scientific investigation. We show in the following section that the variability of SWV in ERA5 is highly consistent with longer time series derived from observations.

3.2 | SWV variability over the tropics

Figure 3a shows the variability of tropical ERA5 SWV anomalies averaged over 15°S–15°N. In the lower stratosphere below 30 km, the anomalies propagate upward, which is similar to the "tape recorder" of the seasonal cycle. In the upper stratosphere above about 30 km, there is no vertical propagation and the phase is almost constant with height. Besides the interannual variability that bears the QBO signature, we can also see a decadal signal: anomalies are positive during the 1980s and 1990s and negative in the 2000s. Figure 3b shows the time series of mean tropical SWV in the lower stratosphere at 15–20 km. The reference from the SDI MIM observation data is shown in Figure 3c. The two time series are consistent with each other, with a high correlation coefficient of 0.85 (over the common period), indicating that the ERA5 data represent the SWV variability very well.

Figure 4 shows the power spectrum of the SWV time series shown in Figure 4b. It depicts statistically significant peaks around 1, 2 and 22 years, with a small shoulder around 5 years. Note, however, that the signal at 22 years should be interpreted with caution given the available sample size. The most pronounced 2-year peak is related to the tropical QBO, which is the dominant interannual time-scale throughout the tropical stratosphere and impacts tropopause temperatures (Baldwin *et al.*, 2001; Diallo *et al.*, 2018). Scaife *et al.* (2003) connected the 5-year peak to the El Niño–Southern Oscillation (ENSO): a positive ENSO anomaly would lead to an SWV increase by affecting the tropopause temperature. The low-frequency variability of SWV is most likely related to low-frequency oscillation from high latitudes such as the Pacific Decadal Oscillation (PDO) and the North Atlantic Oscillation (NAO). These connections are discussed in more detail in sections 3.3 and 3.4.

3.3 | The relationship between tropical SWV and tropical stratospheric processes

It is well documented that the tropical tropopause temperature provides the primary control over its humidity (Brewer, 1949; Fueglistaler *et al.*, 2009; Dessler *et al.*, 2014). This is confirmed by a high correlation between SWV and the temperature around the tropopause (Figure 5). Higher correlations between SWV and the other two variables considered here occur mainly below 40 km: the zonal wind around 30 and 15 km and the vertical component of the residual circulation w* around 25 km are also highly correlated with the tropical SWV, implying an association with the tropical QBO. The high-correlation coefficient at different levels is due to the descending phases of westerly and easterly winds in the lower stratosphere.

Figure 6 shows the vertical structure of variables on interannual time-scales. Figure 6a roughly shows a 2-year signal anomaly for SWV that propagates upward from the lower stratosphere, reflecting the "tape recorder" phenomenon. Meanwhile, the temperature anomaly, the vertical component of the residual circulation w* anomaly and the zonal-mean zonal wind all show a typical downward

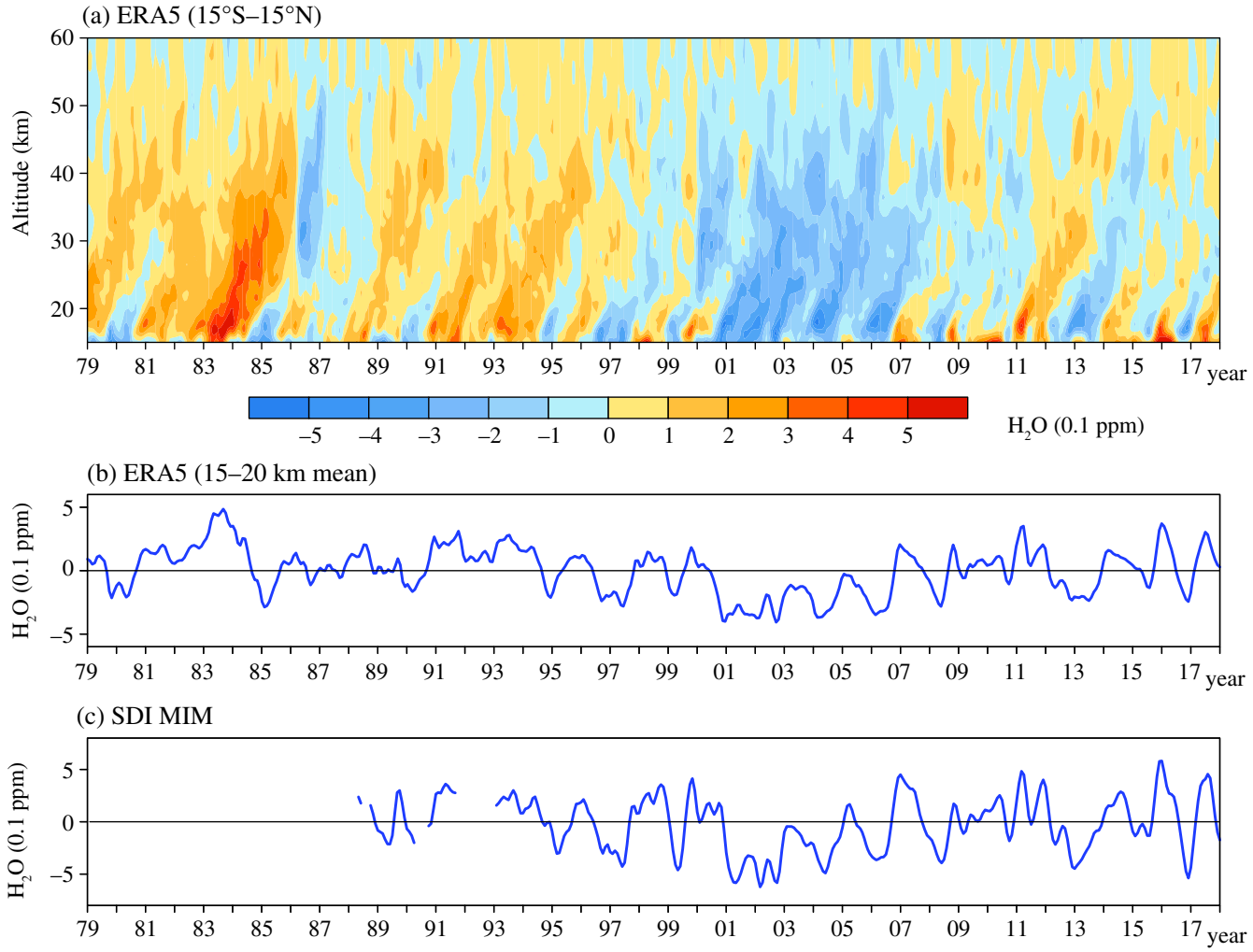

FIGURE 3 Tropical SWV anomalies (15°S–15°N mean) relative to the monthly climatology using (a, b) ERA5 and (c) SDI MIM. The panels (b, c) are based on the 15–20 km mean. Unit: 0.1 ppm

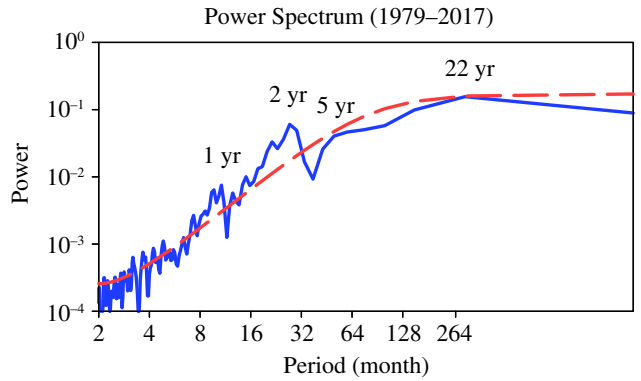

FIGURE 4 Power spectrum of tropical lower-stratospheric water vapour from the ERA5 dataset for the period 1979–2017. The dashed red line indicates the 95% confidence level

propagation of the QBO signal from 40 km (Figure 6b–d). Both theoretical and observational studies have confirmed that the QBO influences the chemical and physical processes in the lower stratosphere. The mean zonal wind and temperature fields during the QBO phases satisfy the thermal wind balance, and the temperature anomaly can be used to analyse the concentration and characteristics of the chemical constituents, such as ozone, methane and water vapour, during the QBO phases (Plumb and Bell, 1982; Baldwin *et al.*, 2001; Holton and Hakim, 2012). Here we seek to analyse and learn about the dynamical process of how the QBO influences the tropical stratospheric circulation and the SWV in the ERA5 data.

The tropical zonal wind at a certain level of the stratosphere can be considered as an index of the QBO phases. Here we take as a reference the zonal wind at 30 km in the middle stratosphere, where the zonal wind contrast is strongest, and choose the months when the westerly/easterly winds are greater than 10 $m \cdot s^{-1}$ as contrast months (Figure 6d). At the same time, the easterly/westerly winds occupy the lower stratosphere, so this month is defined conventionally as the easterly/westerly QBO phase. Based

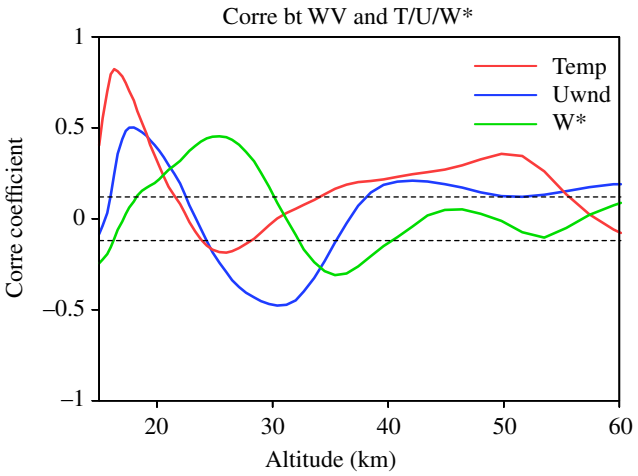

FIGURE 5 Correlation coefficient of tropical lower-stratospheric water vapour with tropical temperature, zonal-mean zonal wind and the vertical component of the residual circulation w* as a function of altitude based on ERA5. The dashed lines indicate the 95% confidence limits

on this classification, we have identified 132 months of easterly QBO (but westerly at 30 km) and 127 months of westerly QBO (but easterly at 30 km) in all seasons during 1979–2017. Figure 7 shows the corresponding composites of circulation and thermal anomalies. During the easterly QBO phase (Figure 7a,c), the descending QBO maintains an easterly zonal wind in the lower stratosphere, as well as warmer temperatures between the overlying westerlies and underlying easterlies due to the thermal wind balance (Figure 7a). Colder temperatures in the lower tropical stratosphere are related to a stronger upwelling from the tropical tropopause. Figure 7c shows the corresponding QBO-induced meridional circulation in the lower stratosphere: an upward motion from the equatorial tropopause and a poleward divergence from tropics to subtropics. Unlike the upwelling in the tropics in the general stratospheric BDC, the motions in the vertical direction of the QBO-induced circulation are different at different levels. Around 30 km, there is divergence in the vertical direction with upwelling and downwelling below and above the westerlies, respectively. The situation is reversed around 20 km, with downwelling and upwelling above and below the easterlies, respectively. This meridional circulation anomaly induced by the QBO westerly phase results in a higher and colder tropical tropopause, and less water vapour entering the tropical stratosphere. Through the poleward motion in the lower stratosphere, the global water vapour is less in the lower stratosphere. The opposite takes place during the QBO easterly phase (Figure 7b,d).

In the extratropics, more symmetrical anomalies are found during the QBO westerly phase (Figure 7b,d): a warmer temperature anomaly and a downward anomaly in the residual circulation in high latitudes in both hemispheres. For the QBO easterly phase (Figure 7a,c), in high latitudes of the Northern Hemisphere the temperature anomaly is warm in the lower stratosphere and cold in the upper stratosphere. The residual circulation anomaly shows an upward motion from the tropical upper stratosphere, poleward to the Northern Hemisphere, and a downward motion in the high latitudes. Both anomalies of temperature and residual circulation show a pattern of enhanced planetary wave activity in the boreal winter. By identifying the season of each month in both the two composite phases, we find that in the QBO easterly phase there are more samples from the boreal winter than from the boreal summer, and the ratio of the associated sample size in DJF to that in JJA is around 1.4. For the QBO westerly phase, the ratio is around 1. This elucidates clearly the observation that, unlike in the westerly phase (Figure 7d), in the easterly phase the residual circulation anomaly reflects a boreal winter-like pattern (Figure 7c). This suggests the existence of an interaction between the tropics (QBO) and the extratropics (e.g., planetary wave activity).

3.4 | The relationship between tropical SWV and the extratropical stratosphere

The meridional circulation of the stratosphere comprises a two-cell structure in the lower stratosphere, with upwelling in the tropics and subsidence in middle and high latitudes, a single cell from the tropics into the winter hemisphere at higher altitudes and a branch from the summer Pole to the winter Pole in the upper stratosphere and mesosphere (Plumb, 2002). The circulation in the tropics is always characterized by an upwelling. In the extratropics, however, it can be reversed in summer and winter seasons. Here we examine the impact of extratropical processes on SWV variability considering different seasons separately.

The climatological annual cycle of the tropical lower-stratospheric water vapour shows a maximum in September and a minimum in February (Figure 8a). There is thus more SWV in the boreal summer than in the boreal winter due to monsoons in the boreal summer (Gettelman *et al.*, 2004). The variability is higher in the boreal winter and lower in the boreal summer (Figure 8b). As for the monthly resolved time series (Figure 3b), the seasonal mean time series (Figure 9) of the tropical SWV anomaly shows substantial interannual variability but also a lower-frequency variation, with more water vapour in the 1980s and early 1990s and less water vapour in the 2000s.

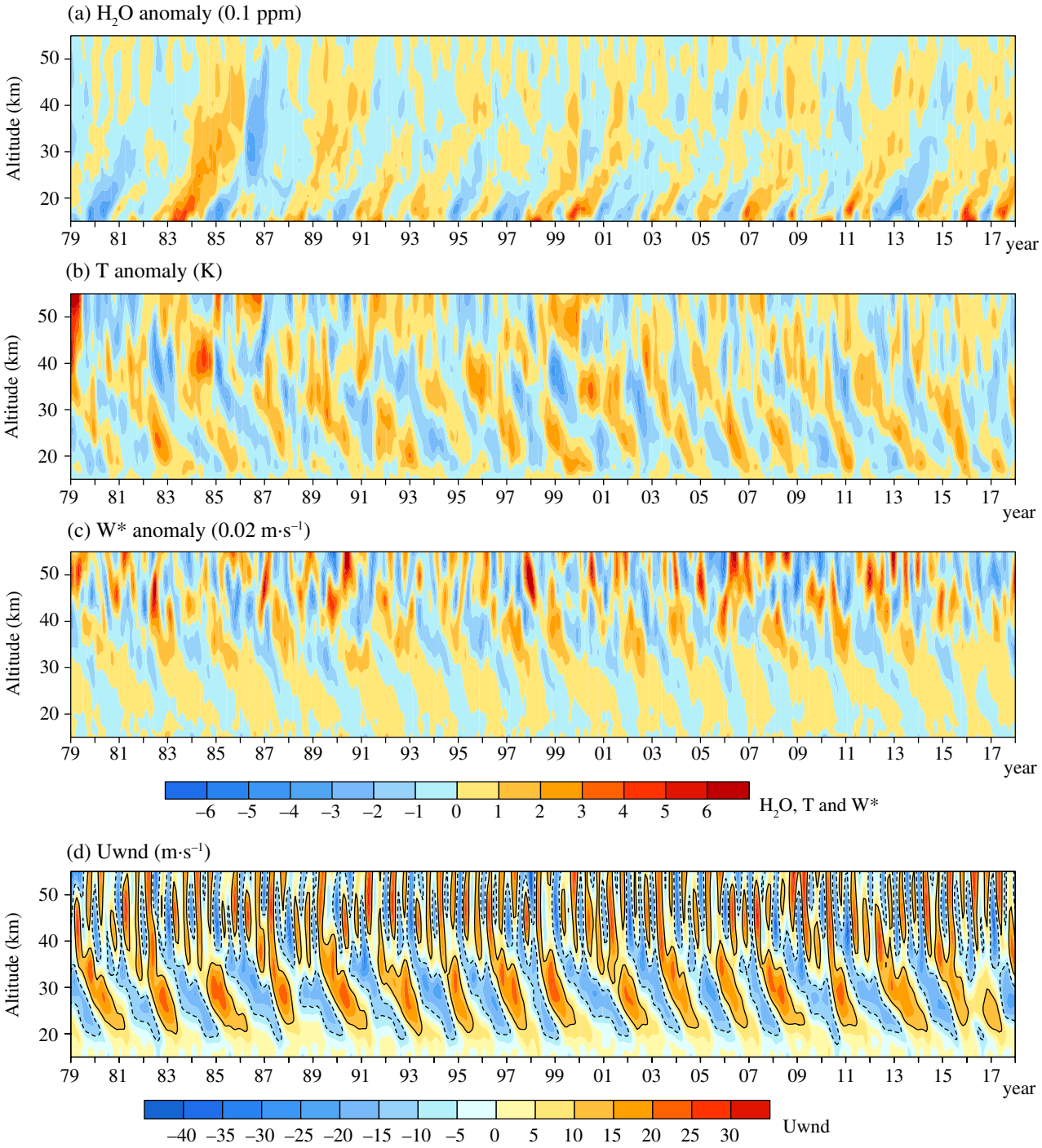

FIGURE 6 Interannual variability (≤ 8 years) in ERA5 tropical mean (15°S–15°N) (a) SWV anomalies (0.1 ppm), (b) temperature anomalies (K), (c) the vertical component of the residual circulation w* anomalies (0.02 m·s^{-1}), and (d) the zonal-mean zonal wind (m·s^{-1}). The solid and dashed lines in (d) represent ± 10 m·s^{-1}. Units for (a–c) share the same colour bar, while the unit for (d) has its own colour bar

Figure 10a,b shows the simultaneous correlation between the tropical lower-stratospheric water vapour (time series in Figure 9) and the temperature at 100 hPa for DJF and JJA, respectively. In the boreal winter, besides the high positive correlation in the tropics and subtropics, there is a significant negative correlation in the winter Pole. This latter correlation is related to the predominant planetary wave number 2 activity, which can be recognized from the climatological circulation (vectors in Figure 10a). There is no such clear planetary wave activity at this level during the austral winter (Figure 10b) because the upward propagation of the planetary wave activity is prohibited by the strong zonal westerly wind (Charney and Drazin, 1961; Wang *et al.*, 2019). This explains the lack

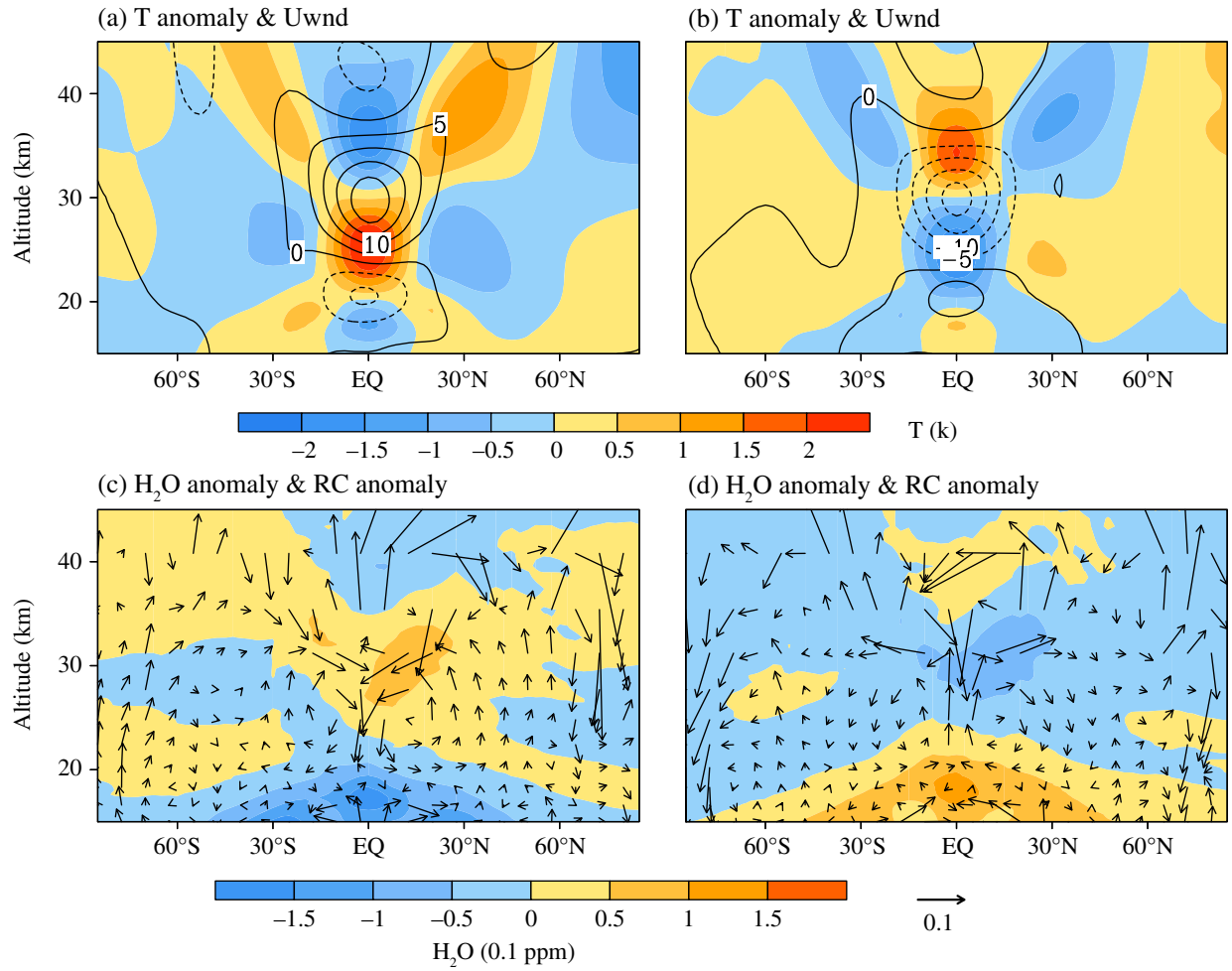

FIGURE 7 Composite of (a, b) temperature anomalies (shading, K) and zonal-mean zonal wind (contours, with intervals of 5 $m \cdot s^{-1}$), (c, d) residual circulation anomalies (vectors) and water vapour anomalies (shading) in the easterly (a, c) and westerly (b, d) QBO phases based on ERA5

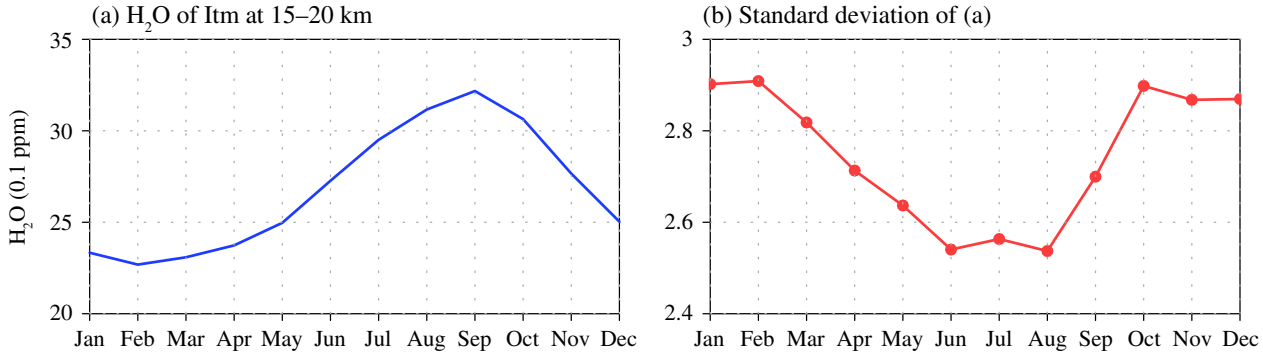

FIGURE 8 ERA5 climatological annual cycle of (a) mean tropical SWV (15°S–15°N mean at 15–20 km) and (b) its standard deviation. Unit: 0.1 ppm

of significant correlation between the tropical SWV and the stratospheric temperature in the austral winter polar region.

This hemispheric difference is shown more clearly in the zonally averaged meridional cross-section of the correlation between the tropical lower-stratospheric water vapour and stratospheric temperature (shading, Figure 10c,d) and the zonal-mean zonal wind (contours, Figure 10c,d). Over the tropics and subtropics there are similar correlations in both seasons: a positive correlation

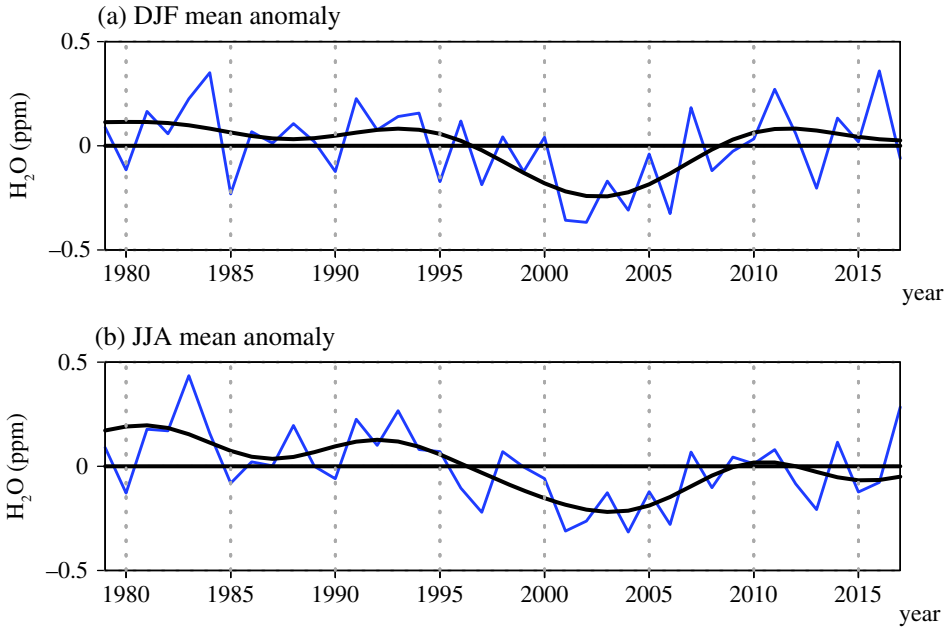

FIGURE 9 Time series of mean tropical SWV anomaly (15°S–15°N mean at 15–20 km) in (a) DJF and (b) JJA. Data is from ERA5

in the lower stratosphere over the tropics and subtropics in the winter hemisphere with temperature, and a negative correlation with tropical zonal wind around 30 km. In high latitudes of the summer hemisphere, there is a positive correlation with temperature around 40–50 km, which is due to new water vapour that is produced from methane oxidation. In high latitudes of the winter hemisphere, in the DJF mean there is a significant positive correlation with the zonal wind and with temperature, while the correlation is negative in the lower stratosphere and positive in the upper stratosphere (Figure 10c). No such significant correlations exist in the high latitudes of the Southern Hemisphere in JJA (Figure 10d). This difference means that, in addition to the tropical processes, the SWV in JJA is solely controlled by methane oxidation over the summer hemisphere. In DJF, on the other hand, besides the methane oxidation, SWV is also affected by planetary wave activities in high latitudes of the winter hemisphere.

In an attempt to get a clearer dynamic picture of the polar circulation effects on the tropical SWV in the boreal winter, based on Figure 9a we select 6 continuous years around the early 1990s (with high SWV) and 6 continuous years starting in 2001 (with low SWV). This period represents a typical decadal feature in the SWV signal. During the period 2001–2006 we can see that the water vapour anomaly is negative not just in the lower stratosphere but in almost the entire stratosphere (Figure 11b). One strong negative anomaly is in the tropics; another is in the winter Pole in the lower stratosphere. The residual circulation anomaly (streamline and v* in Figure 11b and w* in Figure 11d) shows enhanced upward motion from the tropical tropopause and poleward motion to the extratropics in the lower stratosphere, with a stronger winter-poleward flow in the upper stratosphere. This leads to a stronger winter polar downwelling in the middle and lower stratosphere, along with an anomalous polar upwelling in the upper stratosphere. In this case the BDC is enhanced. The zonal wind anomaly structure in the tropics is similar to the QBO westerly phase (Figure 11f), characterized by a westerly anomaly in the middle and upper stratosphere and an easterly anomaly in the lower stratosphere. Meanwhile, in high latitudes of the Northern Hemisphere there is a strong easterly anomaly across the depth of the stratosphere, a warm temperature anomaly in the lower and middle stratosphere, and a cold anomaly in the upper stratosphere (Figure 11d). This is concurrent with a weakening of the polar vortex, which is favourable for the downwelling in the polar region in the lower stratosphere. The downwelling, together with the enhanced poleward flow, brings about a stronger tropical upwelling and poleward divergence in the lower stratosphere (Figure 11b,d). The stronger tropical upwelling results in a colder tropical tropopause and leads to cold temperature anomalies in the lower tropical and subtropical stratosphere. This is consistent with less water in the stratosphere, in which the easterly anomaly in the polar zonal wind and the warm anomaly in the polar temperature in the lower and middle stratosphere are due to a strong upward propagation of planetary wave activity (Figure 11f). As is typically observed during SSWs, warming anomalies in the lower and middle stratosphere are generally accompanied by cooling anomalies above them (Andrews *et al.*, 1987; Holton and Hakim, 2012), caused by the upward anomaly motion (or significantly weakened downward motion) in the polar upper stratosphere (Figure 11b,d).

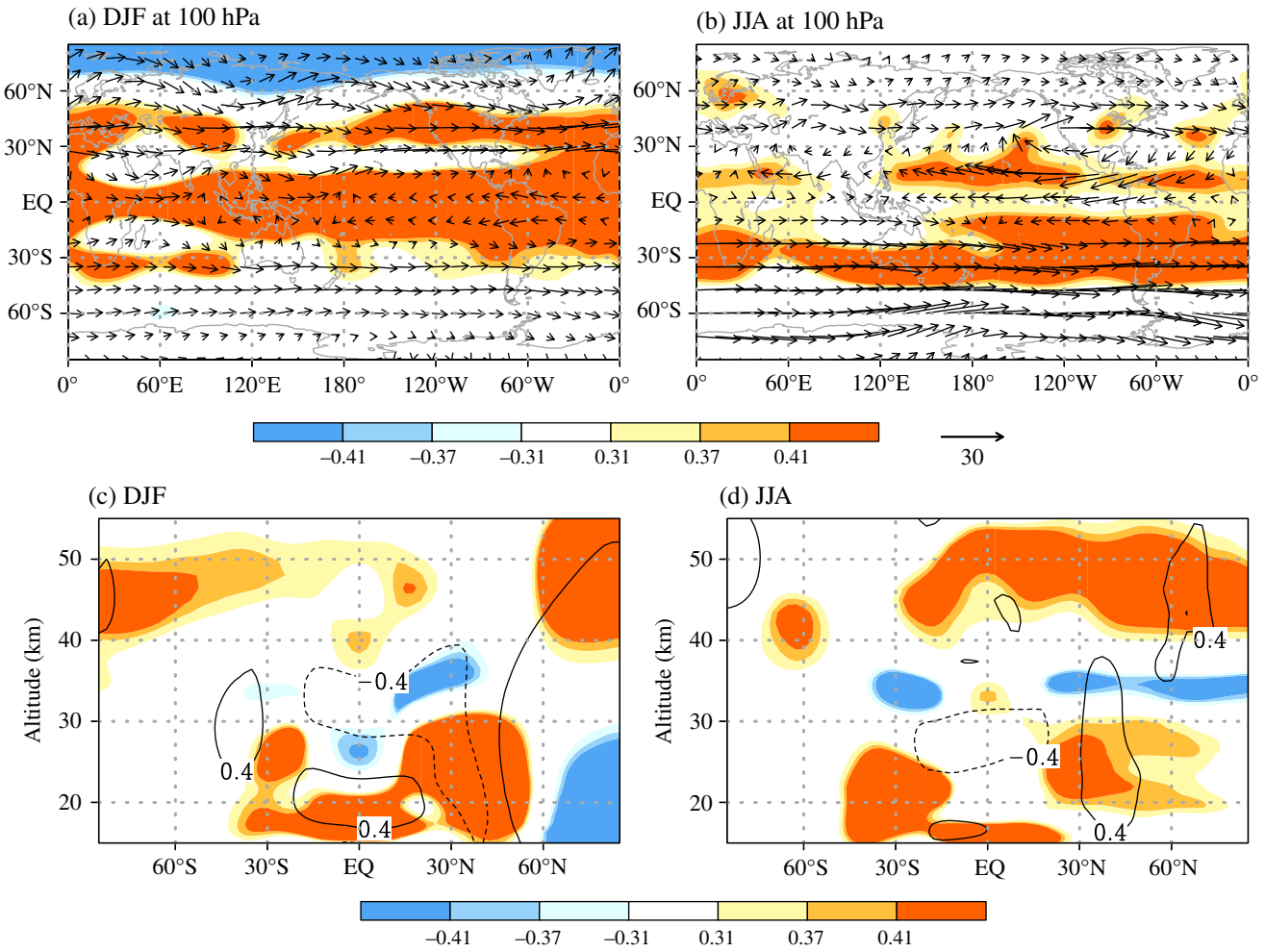

FIGURE 10 Correlation coefficient between (ERA5) tropical lower-stratospheric water vapour (15°S–15°N averaged at 15–20 km) and 100-hPa-horizontal (a, b) zonally averaged meridional, (c, d) temperature field (shading). The contour shown in (c, d) is the correlation between tropical SWV and zonal-mean zonal wind. The 99% confidence interval is shown as ±0.4. The climatological circulation at 100 hPa is shown as vectors in (a, b)

The positive anomaly of the vertical wave activity flux in Northern Hemisphere high latitudes is an indication of the influence of planetary wave activity on the circulation. Stronger upward-propagating planetary wave activity leads to the release of more easterly momentum. This can induce a deceleration of the westerly wind and/or a poleward meridional wind (Andrews *et al.*, 1987). Meanwhile the lower- (upper-) stratospheric polar region becomes warmer (colder) due to the frequency of SSWs in this period (Butler *et al.*, 2017). A composite analysis of SSWs from a previous study revealed that the meridional circulation change associated with SSWs in the polar region produces a temperature decrease in the equatorial lower stratosphere (Kodera, 2006), which is consistent with Figure 11b,d,f.

In comparison, the period 1991–1996, which is associated with a positive tropical SWV anomaly (Figure 9a), shows the opposite picture, especially in the winter polar region. More water vapour is observed in the entire stratosphere, with a particularly strong positive anomaly in the winter Pole (Figure 11a) and a westerly anomaly in the polar wind, with a cold anomaly in lower-stratospheric temperature (Figure 11c,e). In addition, there is a downwelling anomaly in the tropics and an upwelling anomaly in the lower-stratospheric winter Pole (Figure 11c), which are consistent with the weaker upward propagation of planetary wave activity (fewer SSWs) over Northern Hemisphere high latitudes (Figure 11e). Butler *et al.* (2017) show that there was no major SSW event during the winter of 1991–1996, whereas in 2001–2006 there was at least one major SSW event each winter.

On decadal time-scales, Omrani *et al.* (2014) showed that large-scale Atlantic warming associated with Atlantic Multidecadal Variability (AMV) drives high-latitude precursory stratospheric warmings in early to mid-winter that propagate downward resulting in a negative North Atlantic

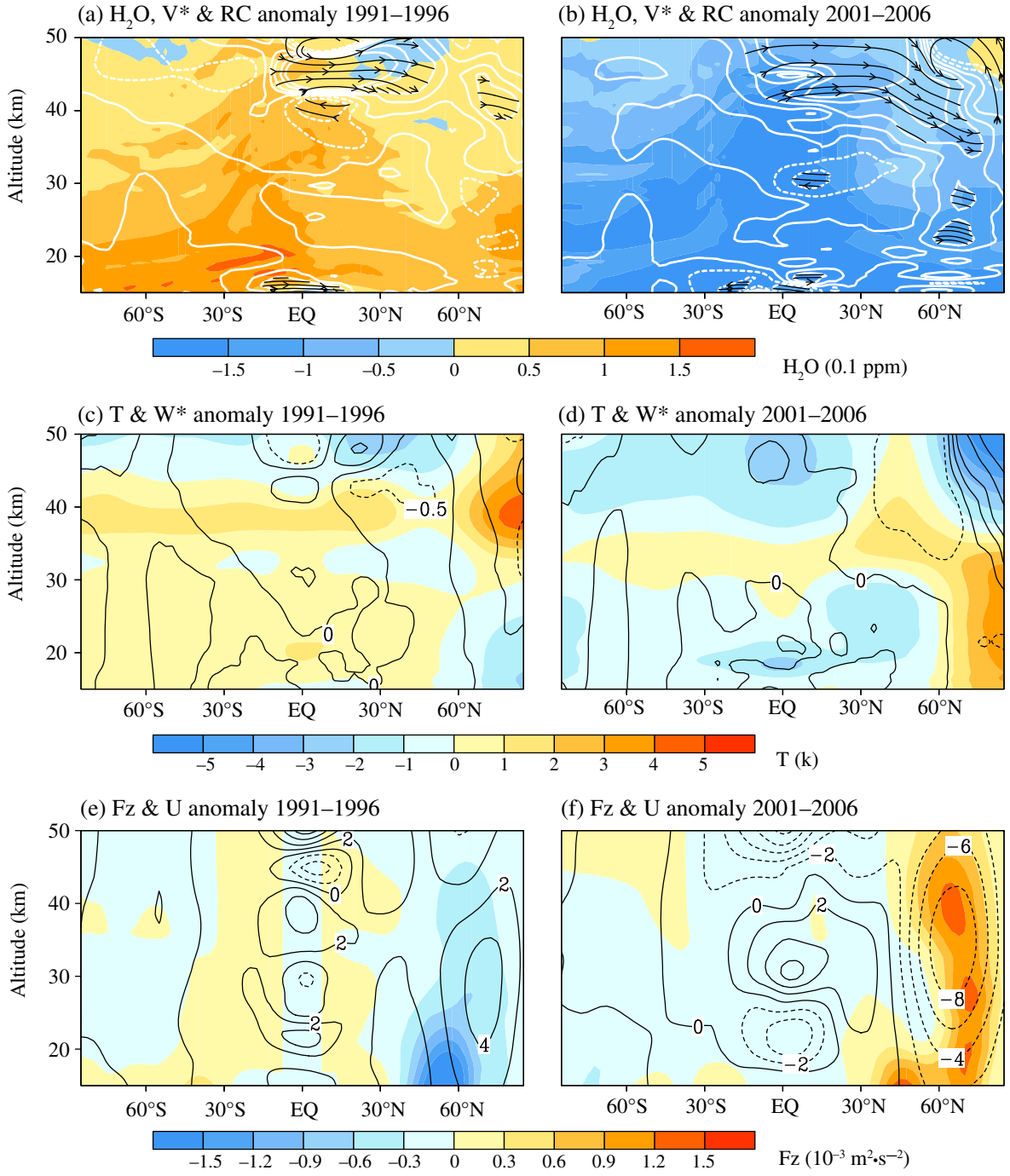

FIGURE 11 Composite of (a, b) water vapour (shading), residual circulation (streamline) and v* (contour) anomalies; (c, d) the vertical velocity of residual circulation w* (contour) and temperature (shading) anomalies; and (e, f) zonal-mean zonal wind (contour) and the vertical component of planetary wave activity flux (shading) anomalies over the ERA5 period 1991–1996 (a, c, e) and 2001–2006 (b, d, f)

Oscillation (NAO) in late winter. The SST composite analysis shows a significant anomaly over the North Atlantic, with a strong positive anomaly during 2001–2006 and a negative anomaly during 1991–1996 (Figure 12). The correlation between the tropical SWV and the North Atlantic SST on decadal time-scales is −0.7. It is also highly correlated with the NAO index. One possible mechanism of the influence of the North Atlantic SST on SWV can be explained by the fact that the warmer North Atlantic (associated with the warm phase of AMV) in winter provides an enhancement to the thermal contrast between land and sea. This may force stronger planetary wave activity, which then affects the thermal and dynamical conditions in the stratosphere (a warmer high-latitude stratosphere in the Northern Hemisphere and a stronger BDC). This mechanism is consistent with the study of

Omrani *et al.* (2014). Another possible mechanism is the link between the AMV phase and the frequency of North Atlantic blocking. The occurrence of blockings is associated with the warm phase of AMV (Häkkinen *et al.*, 2011), which modulates the upward planetary wave propagation (Nishii *et al.*, 2011).

Another significant anomaly in Figure 12a is the PDO-like anomaly in the North Pacific, but it is not robust in Figure 12b. Other opposite anomalies in these two periods can be seen around the warm pool in the Western Pacific and east of the dateline in the South Pacific around 30°S. The SST anomalies in these regions can have non-negligible impacts on convection, which can then influence the tropopause temperature and the water vapour entering the stratosphere.

4 | DISCUSSION

In the previous section, a composite analysis was conducted based on the variability of tropical water vapour in the lower stratosphere and its relationship to the dynamical variables in the tropics and polar regions. On interannual time-scales, during the tropical QBO westerly or easterly phases, the tropical water vapour anomaly is consistent with the global water vapour in the lower stratosphere (Figure 7c,d). Meanwhile, on decadal time-scales the tropical water vapour exhibits the same tendency in the entire stratosphere (Figure 11a,b). Furthermore, on interannual time-scales the main meridional circulation anomaly exhibits a two-cell structure in the lower stratosphere, with upwelling in the tropics and subsidence in middle and high latitudes (Figure 7). This circulation affects the anomaly of global water vapour in the lower stratosphere. On decadal time-scales, as shown in Figure 11, besides the tropical anomaly in the lower stratosphere, the residual circulation anomaly shows up as a single cell extending from the tropics into the winter Pole in the upper stratosphere, which is connected to planetary wave activity. This circulation anomaly affects water vapour not only in the lower stratosphere but also in the upper stratosphere.

In this work, we have investigated in particular the effects of the QBO on the interannual variability of SWV and the influence of planetary wave activity (and stratospheric warmings) on the decadal variability of SWV during the boreal winter. During periods of low SWV anomalies (Figure 11f), when the upward propagation of planetary waves is stronger (with a weaker polar vortex), the tropical zonal wind anomaly is similar to the zonal wind pattern shown in Figure 7a, namely that for the easterly QBO phase. This is consistent with the Holton–Tan relationship (Holton and Tan, 1980): during the easterly QBO phase, the propagation of planetary waves is more poleward and the stratospheric polar vortex is weaker. This relationship to the QBO, on interannual time-scales, has been well investigated in previous observational and numerical studies (Holton and Tan, 1982; Naito *et al.*, 2003; Anstey and Shepherd, 2014; Gómez-Escolar *et al.*, 2014; Koval *et al.*, 2018). The effect of the QBO on the northern stratospheric polar vortex has decadal changes (Lu *et al.*, 2008). Here we also reveal that the extratropical anomaly pattern in the easterly QBO phase is an enhanced planetary wave activity pattern in the boreal winter (Figure 7a, c), similar to what appears in the low SWV decadal period. More challenging questions, however, remain to be answered and require further investigation, namely (i) "What is the connection between the QBO and the decadal oscillation?" and (ii) "What is the dynamical mechanism of the QBO impact on the SWV decadal variability?"

Both the monthly and seasonal mean tropical SWV anomalies (Figures 3 and 9) show an abrupt drop from 2000. The abundance of tropical lower-stratospheric water vapour is mostly affected by temperature variations and the tropical upwelling (e.g., Rosenlof and Reid, 2008; Fueglistaler *et al.*, 2009). It suggests that the tropical SSTs may contribute to the abundance of water vapour brought to the stratosphere via convection in the troposphere and the temperature of the tropopause (e.g., Randel *et al.*, 2006; Brinkop *et al.*, 2016; Garfinkel *et al.*, 2018). Brinkop *et al.* (2016) found that the driving forces for this water vapour drop are changes due to coincidence with a preceding strong El Niño event (1997–1998), followed by a strong La Niña event (1999–2000) and supported by the phase change of the QBO in 2000. Ding and Fu (2018) suggest that the tropical central Pacific SST could contribute to the stepwise drop of the lower-stratospheric water vapour from 1992–2000 to 2001–2005. Other studies investigated the anomalous SWV during the unusual El Niño event of 2015–2016 and found that the strong El Niño aligned with a disrupted QBO caused tropical lower-stratospheric water vapour to increase (Avery *et al.*, 2017; Diallo *et al.*, 2018). This disruption of the QBO is also observed in ERA5 (see Figure 6). Wang *et al.* (2017) found weak correlations between the tropical SWV and SST anomalies on interannual time-scales. Solomon *et al.* (2010) show that the tropical SWV is negatively correlated with the warm pool SST in the Pacific. With ERA5 data, a linear correlation shows that, on decadal time-scales, the tropical lower-stratospheric water vapour is significantly negatively correlated with the warm pool and the North Atlantic SST (see section 3). On interannual time-scales the correlation is weak. A thorough understanding of these correlation structures goes beyond the scope of this paper and is left for future research.

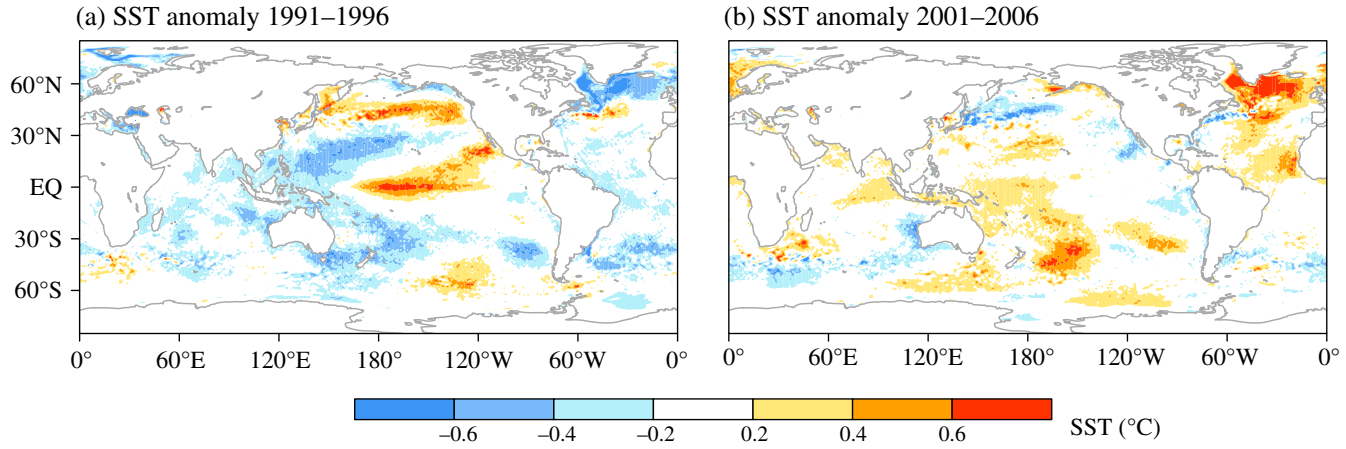

FIGURE 12 Composite of ERA5 sea-surface temperature (SST) anomalies over the periods (a) 1991–1996 and (b) 2001–2006

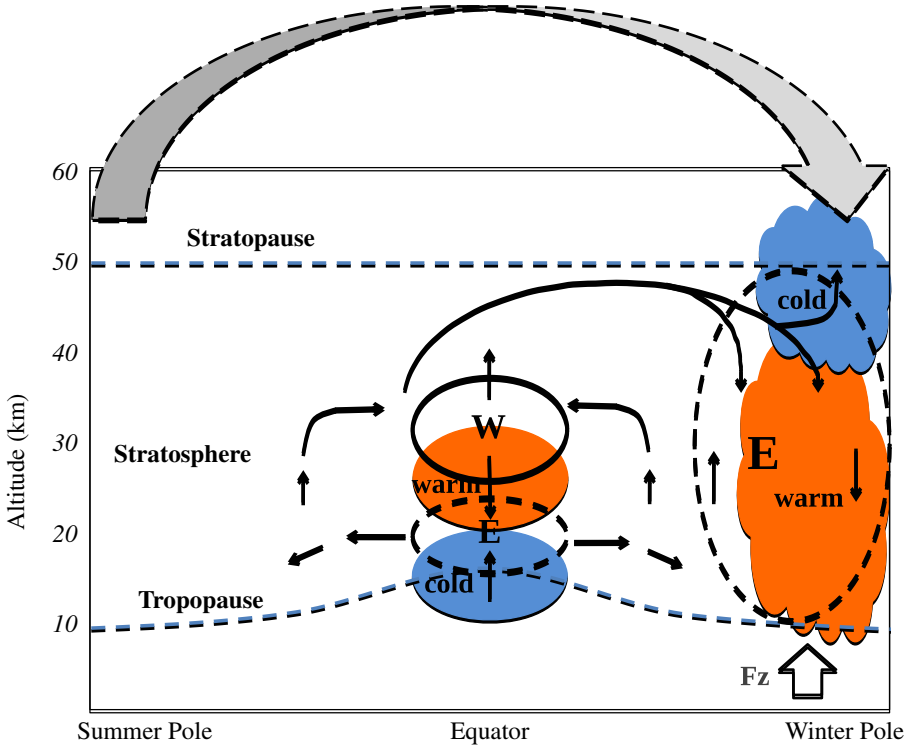

FIGURE 13 Schematic representation of the dynamic mechanism relating the QBO, planetary wave activity, and a plausible gravity wave change to SWV. The mesospheric branch of the meridional circulation is weakened by suppressed vertical propagation of gravity waves with easterly momentum due to the appearance of easterlies in the winter hemisphere. Refer to the text for more details

5 | CONCLUSIONS

In this work, we have compared two SWV products from ECMWF, namely the recently released reanalysis product ERA5 and its predecessor, ERA-Interim, along with multi-instrument mean observations from the SPARC Data Initiative (SDI MIM). The comparison is based on the seasonal mean climatology and variability of SWV in the tropics and high latitudes. The results show that in ERA5 SWV has a very good climatological representation of the seasonal mean and the variability in SWV is better represented in ERA5 than in ERA-Interim, especially in the upper stratosphere. The variability of tropical water vapour in the lower stratosphere in ERA5 is highly consistent with that in the SDI MIM observations. ERA5 describes the stratospheric oscillations in the tropics (e.g., QBO, SAO) and variability in the extratropics very well, and it has great potential to be used for investigations into stratospheric dynamics.

Based on the ERA5 dataset spanning the period 1979–2017, the variability of tropical SWV and its relation to tropical and extratropical dynamic processes are investigated. The tropical water vapour in the lower stratosphere shows significant frequencies of the order of 1, 2 and

22 years. A Fourier analysis is used to separate the variability into interannual and decadal time-scales. Composite analyses based on interannual QBO phases and two typical decadal SWV periods (with low and high anomalies) are conducted to investigate the mechanism of the influence of stratospheric processes on SWV. The relationship between the tropical SWV and tropical dynamical variables is dominated mostly by interannual time-scales and is related to the tropical QBO. The mechanism is represented schematically in Figure 13. During the easterly QBO phase, the stronger upwelling in the lower stratosphere results in a colder tropical tropopause, which leads to a stronger dehydration and a negative water vapour anomaly in the stratosphere. Such dry air would extend to the entire lower stratosphere with an eventual poleward transport.

On decadal time-scales, the North Atlantic SST anomaly influences the SWV by affecting the upward propagation of planetary waves and the stratospheric residual circulation in the boreal winter. The warmer North Atlantic SST thus enhances the planetary wave activity. As shown in Figure 13, stronger upward propagating planetary wave activity leads to a warmer winter polar region in the lower to middle stratosphere and a weaker polar vortex and/or a stronger BDC. The tropical upwelling is therefore stronger and the tropical tropopause is colder, leading to less water vapour entering the stratosphere, with this negative anomaly extending throughout the stratosphere while the air is distributed within the large-scale residual circulation. On the other hand, cold anomalies in the upper polar stratosphere could be caused by the anomalous polar upwelling, and may also be influenced by a weakened mesospheric branch of the meridional circulation due to reduced gravity wave activity with easterly momentum, which easterlies in the winter stratosphere might prevent from vertically propagating into the mesosphere.

ACKNOWLEDGEMENTS

This work is jointly funded by the Swedish National Space Board project Dnr 88/11 “Atmospheric modelling using space-based observations of stable water isotopes” and the Department of Meteorology, Stockholm University. T. H. was funded by the International Meteorological Institute (IMI) of Stockholm University, and was also supported by KAKENHI Grant numbers JP16H04052, JP17H01159, JP18H01280 and JP18H01270. The ERA5 data were downloaded from the ECMWF website. The data analyses were performed on resources provided by the Swedish National Infrastructure for Computing (SNIC) at the National Supercomputer Center (NSC). Two anonymous reviewers provided constructive comments that helped to improve the manuscript.

ORCID

Tongmei Wang https://orcid.org/0000-0002-2557-8541

REFERENCES

Andrews, D.G., Holton, J.R. and Leovy, C.B. (1987) *Middle Atmosphere Dynamics*, Vol. 40. Orland, CA: Academic Press.

Anstey, J.A. and Shepherd, T.G. (2014) High-latitude influence of the quasi-biennial oscillation. *Quarterly Journal of the Royal Meteorological Society*, 140(678), 1–21.

Avery, M.A., Davis, S.M., Rosenlof, K.H., Ye, H. and Dessler, A.E. (2017) Large anomalies in lower stratospheric water vapour and ice during the 2015–2016 El Niño. *Nature Geoscience*, 10(6), 405–409.

Baldwin, M.P., Gray, L.J., Dunkerton, T.J., Hamilton, K., Haynes, P.H., Randel, W.J., Holton, J.R., Alexander, M.J., Hirota, I., Horinouchi, T., Jones, D.B.A., Kinnersley, J.S., Marquardt, C., Sato, K. and Takahashi, M. (2001) The quasi-biennial oscillation. *Reviews of Geophysics*, 39(2), 179–229.

Brewer, A.W. (1949) Evidence for a world circulation provided by the measurements of helium and water vapour distribution in the stratosphere. *Quarterly Journal of the Royal Meteorological Society*, 75(326), 351–363.

Brinkop, S., Dameris, M., Joeckel, P., Garny, H., Lossow, S. and Stiller, G. (2016) The millennium water vapour drop in chemistry–climate model simulations. *Atmospheric Chemistry and Physics*, 16(13), 8125–8140.

Butler, A.H., Sjoberg, J.P., Seidel, D.J. and Rosenlof, K.H. (2017) A sudden stratospheric warming compendium. *Earth System Science Data*, 9(1), 63–76.

Charney, J.G. and Drazin, P.G. (1961) Propagation of planetary-scale disturbances from the lower into the upper atmosphere. *Journal of Geophysical Research*, 66, 83–109.

Copernicus Climate Change Service (C3S) (2017) ERA5: fifth generation of ECMWF atmospheric reanalyses of the global climate. Available at: https://cds.climate.copernicus.eu/cdsapp#!/home [Accessed 22nd January 2019].

Davis, S.M., Hegglin, M.I., Fujiwara, M., Dragani, R., Harada, Y., Kobayashi, C., Long, C., Manney, G.L., Nash, E.R., Potter, G.L., Tegtmeier, S., Wang, T., Wargan, K. and Wright, J.S. (2017) Assessment of upper tropospheric and stratospheric water vapor and ozone in reanalyses as part of S-RIP. *Atmospheric Chemistry and Physics*, 17(20), 12743–12778.

Dee, D.P., Uppala, S.M., Simmons, A.J., Berrisford, P., Poli, P., Kobayashi, S., Andrae, U., Balmaseda, M.A., Balsamo, G., Bauer, P., Bechtold, P., Beljaars, A.C.M., van de Berg, L., Bidlot, J., Bormann, N., Delsol, C., Dragani, R., Fuentes, M., Geer, A.J., Haimberger, L., Healy, S.B., Hersbach, H., Hólm, E.V., Isaksen, L., Kållberg, P., Köhler, M., Matricardi, M., McNally, A.P., Monge-Sanz, B.M., Morcrette, J.J., Park, B.K., Peubey, C., de Rosnay, P., Tavolato, C., Thépaut, J.N. and Vitart, F. (2011) The ERA-Interim reanalysis: configuration and performance of the data assimilation system. *Quarterly Journal of the Royal Meteorological Society*, 137(656), 553–597. https://doi.org/10.1002/qj.828

Dessler, A.E., Schoeberl, M.R., Wang, T., Davis, S.M. and Rosenlof, K.H. (2013) Stratospheric water vapor feedback. *Proceedings of the National Academy of Sciences*, 110(45), 18087–18091.

Dessler, A.E., Schoeberl, M.R., Wang, T., Davis, S.M., Rosenlof, K.H. and Vernier, J.P. (2014) Variations of stratospheric water vapor

over the past three decades. *Journal of Geophysical Research: Atmospheres*, 119(22), 12588–12598.

Dethof, A. and Hólm, E.V. (2004) Ozone assimilation in the ERA-40 reanalysis project. *Quarterly Journal of the Royal Meteorological Society*, 130(603), 2851–2872.

Diallo, M., Riese, M., Birner, T., Konopka, P., Müller, R., Hegglin, M.I., Santee, M.L., Baldwin, M., Legras, B. and Ploeger, F. (2018) Response of stratospheric water vapor and ozone to the unusual timing of El Niño and the QBO disruption in 2015–2016. *Atmospheric Chemistry and Physics*, 18(17), 13055–13073.

Ding, Q. and Fu, Q. (2018) A warming tropical central Pacific dries the lower stratosphere. *Climate Dynamics*, 50(7–8), 2813–2827.

Dvortsov, V.L. and Solomon, S. (2001) Response of the stratospheric temperatures and ozone to past and future increases in stratospheric humidity. *Journal of Geophysical Research: Atmospheres*, 106(D7), 7505–7514.

Eichinger, R., Jöckel, P. and Lossow, S. (2015) Simulation of the isotopic composition of stratospheric water vapour – part 2: investigation of HDO/H_2O variations. *Atmospheric Chemistry and Physics*, 15(12), 7003–7015.

Forster, P.M.d.F. and Shine, K.P. (1999) Stratospheric water vapour changes as a possible contributor to observed stratospheric cooling. *Geophysical Research Letters*, 26(21), 3309–3312.

Forster, P.M.d.F. and Shine, K.P. (2002) Assessing the climate impact of trends in stratospheric water vapor. *Geophysical Research Letters*, 29(6), 10–11.

Fueglistaler, S., Dessler, A.E., Dunkerton, T.J., Folkins, I., Fu, Q. and Mote, P.W. (2009) Tropical tropopause layer. *Reviews of Geophysics*, 47(1), 1–31.

Garfinkel, C.I., Gordon, A., Oman, L.D., Li, F., Davis, S. and Pawson, S. (2018) Nonlinear response of tropical lower-stratospheric temperature and water vapor to ENSO. *Atmospheric Chemistry and Physics*, 18, 4597–4615.

Gettelman, A., Kinnison, D.E., Dunkerton, T.J. and Brasseur, G.P. (2004) Impact of monsoon circulations on the upper troposphere and lower stratosphere. *Journal of Geophysical Research: Atmospheres*, 109(D22), D22101.

Gómez-Escolar, M., Calvo, N., Barriopedro, D. and Fueglistaler, S. (2014) Tropical response to stratospheric sudden warmings and its modulation by the QBO. *Journal of Geophysical Research: Atmospheres*, 119(12), 7382–7395.

Häkkinen, S., Rhines, P.B. and Worthen, D.L. (2011) Atmospheric blocking and Atlantic multidecadal ocean variability. *Science*, 334(6056), 655–659.

Hegglin, M.I., Plummer, D.A., Shepherd, T.G., Scinocca, J.F., Anderson, J., Froidevaux, L., Funke, B., Hurst, D., Rozanov, A., Urban, J., von Clarmann, T., Walker, K.A., Wang, H.J., Tegtmeier, S. and Weigel, K. (2014) Vertical structure of stratospheric water vapour trends derived from merged satellite data. *Nature Geoscience*, 7(10), 768–776.

Hegglin, M.I., Tegtmeier, S., Anderson, J., Froidevaux, L., Fuller, R., Funke, B., Jones, A., Lingenfelser, G., Lumpe, J., Pendlebury, D., Remsberg, E., Rozanov, A., Toohey, M., Urban, J., von Clarmann, T., Walker, K.A., Wang, R. and Weigel, K. (2013) SPARC data initiative: comparison of water vapor climatologies from international satellite limb sounders. *Journal of Geophysical Research: Atmospheres*, 118(20), 11–824.

Hersbach H, P. de Rosnay, B. Bell, D. Schepers, A. Simmons, C. Soci, S. Abdalla, M. Alonso Balmaseda, G. Balsamo, P. Bechtold, P. Berrisford, J. Bidlot, E. de Boisséson, M. Bonavita, P. Browne, R. Buizza, P. Dahlgren, D. Dee, R. Dragani, M. Diamantakis, J. Flemming, R. Forbes, A. Geer, T. Haiden, E. Hólm, L. Haimberger, R. Hogan, A. Horányi, M. Janisková, P. Laloyaux, P. Lopez, J. Muñoz-Sabater, C. Peubey, R. Radu, D. Richardson, J.-N. Thépaut, F. Vitart, X. Yang, E. Zsótér & H. Zuo, (2018) *Operational global reanalysis: progress, future directions and synergies with NWP*, ECMWF ERA Report 27.

Holton, J.R. and Hakim, G.J. (2012) *An Introduction to Dynamic Meteorology*, Vol. 88. Waltham, MA: Elsevier Academic Press, p. 552.

Holton, J.R., Haynes, P.H., McIntyre, M.E., Douglass, A.R., Rood, R.B. and Pfister, L. (1995) Stratosphere-troposphere exchange. *Reviews of Geophysics*, 33(4), 403–439.

Holton, J.R. and Tan, H.C. (1980) The influence of the equatorial quasi-biennial oscillation on the global circulation at 50 mb. *Journal of the Atmospheric Sciences*, 37(10), 2200–2208.

Holton, J.R. and Tan, H.C. (1982) The quasi-biennial oscillation in the Northern Hemisphere lower stratosphere. *Journal of the Meteorological Society of Japan Series II*, 60(1), 140–148.

Hoskins, B.J. (1991) Towards a PV-θ view of the general circulation. *Tellus A*, 43(4), 27–36.

Jackson, D.R., Burrage, M.D., Harries, J.E., Gray, L.J. and Russell, J., III. (1998) The semi-annual oscillation in upper stratospheric and mesospheric water vapour as observed by HALOE. *Quarterly Journal of the Royal Meteorological Society*, 124, 2493–2515.

Kodera, K. (2006) Influence of stratospheric sudden warming on the equatorial troposphere. *Geophysical Research Letters*, 33(6), L06804.

Koval, A.V., Gavrilov, N.M., Pogoreltsev, A.I. and Savenkova, E.N. (2018) Comparisons of planetary wave propagation to the upper atmosphere during stratospheric warming events at different QBO phases. *Journal of Atmospheric and Solar-Terrestrial Physics*, 171, 201–209.

Lu, H., Baldwin, M.P., Gray, L.J. and Jarvis, M.J. (2008) Decadal-scale changes in the effect of the QBO on the northern stratospheric polar vortex. *Journal of Geophysical Research: Atmospheres*, 113(D10), 1–14.

Mote, P.W., Rosenlof, K.H., McIntyre, M.E., Carr, E.S., Gille, J.C., Holton, J.R., Kinnersley, J.S., Pumphrey, H.C., Russell, J.M., III and Waters, J.W. (1996) An atmospheric tape recorder: the imprint of tropical tropopause temperatures on stratospheric water vapor. *Journal of Geophysical Research: Atmospheres*, 101(D2), 3989–4006.

Naito, Y., Taguchi, M. and Yoden, S. (2003) A parameter sweep experiment on the effects of the equatorial QBO on stratospheric sudden warming events. *Journal of the Atmospheric Sciences*, 60(11), 1380–1394.

Nishii, K., Nakamura, H. and Orsolini, Y.J. (2011) Geographical dependence observed in blocking high influence on the stratospheric variability through enhancement and suppression of upward planetary-wave propagation. *Journal of Climate*, 24(24), 6408–6423.

Omrani, N.E., Keenlyside, N.S., Bader, J. and Manzini, E. (2014) Stratosphere key for wintertime atmospheric response to warm Atlantic decadal conditions. *Climate Dynamics*, 42(3–4), 649–663.

Orsolini, Y.J., Urban, J., Murtagh, D.P., Lossow, S. and Limpasuvan, V. (2010) Descent from the polar mesosphere and anomalously high stratopause observed in 8 years of water vapor and temperature satellite observations by the Odin Sub-Millimeter

Radiometer. *Journal of Geophysical Research: Atmospheres*, 115(D12), D12305.

Plumb, R.A. (1985) On the three-dimensional propagation of stationary waves. *Journal of the Atmospheric Sciences*, 42(3), 217–229.

Plumb, R.A. (2002) Stratospheric transport. *Journal of the Meteorological Society of Japan Series II*, 80(4B), 793–809.

Plumb, R.A. and Bell, R.C. (1982) A model of the quasi-biennial oscillation on an equatorial beta-plane. *Quarterly Journal of the Royal Meteorological Society*, 108, 335–352.

Randel, W.J., Wu, F., Voemel, H., Nedoluha, G.E. and Forster, P. (2006) Decreases in stratospheric water vapor after 2001: Links to changes in the tropical tropopause and the Brewer-Dobson circulation. *Journal of Geophysical Research: Atmospheres*, 111(D12), 1–11.

Riese, M., Ploeger, F., Rap, A., Vogel, B., Konopka, P., Dameris, M. and Forster, P. (2012) Impact of uncertainties in atmospheric mixing on simulated UTLS composition and related radiative effects. *Journal of Geophysical Research: Atmospheres*, 117(D16), D16305.

Rosenlof, K.H. and Reid, G.C. (2008) Trends in the temperature and water vapor content of the tropical lower stratosphere: sea surface connection. *Journal of Geophysical Research: Atmospheres*, 113(D6), D06107.

Scaife, A.A., Butchart, N., Jackson, D.R. and Swinbank, R. (2003) Can changes in ENSO activity help to explain increasing stratospheric water vapor? *Geophysical Research Letters*, 30(17), 1880–1883.

Shepherd, T.G. (2007) Transport in the middle atmosphere. *Journal of the Meteorological Society of Japan*, 85B, 165–191.

Solomon, S., Rosenlof, K.H., Portmann, R.W., Daniel, J.S., Davis, S.M., Sanford, T.J. and Plattner, G.K. (2010) Contributions of stratospheric water vapor to decadal changes in the rate of global warming. *Science*, 327(5970), 1219–1223.

Steinwagner, J., Fueglistaler, S., Stiller, G., Von Clarmann, T., Kiefer, M., Borsboom, P.-P., van Delden, A.J. and Röckmann, T. (2010) Tropical dehydration processes constrained by the seasonality of stratospheric deuterated water. *Nature Geoscience*, 3(4), 262–266.

Vogel, B., Feck, T. and Grooß, J.U. (2011) Impact of stratospheric water vapor enhancements caused by CH_4 and H_2O increase on polar ozone loss. *Journal of Geophysical Research: Atmospheres*, 116(D5), D05301.

Wang, T., Zhang, Q., Hannachi, A., Lin, Y. and Hirooka, T. (2019) On the dynamics of the spring seasonal transition in the two hemispheric high-latitude stratosphere. *Tellus A*, 71(1), 1634949.

Wang, T., Zhang, Q., Lossow, S., Chafik, L., Risi, C., Murtagh, D. and Hannachi, A. (2018) Stable Water Isotopologues in the stratosphere retrieved from Odin/SMR measurements. *Remote Sensing*, 10(2), 166.

Wang, Y., Su, H., Jiang, J.H., Livesey, N.J., Santee, M.L., Froidevaux, L., Read, W.G. and Anderson, J. (2017) The linkage between stratospheric water vapor and surface temperature in an observation-constrained coupled general circulation model. *Climate Dynamics*, 48(7–8), 2671–2683.

How to cite this article: Wang T, Zhang Q, Hannachi A, Hirooka T, Hegglin MI. Tropical water vapour in the lower stratosphere and its relationship to tropical/extratropical dynamical processes in ERA5. *Q J R Meteorol Soc*. 2020;1–18. https://doi.org/10.1002/qj.3801